IGNITION AND PROPERTIES OF RF CAPACITIVE DISCHARGE IN ACETYLENE

V.A. Lisovskiy, S.V. Dudin, P.P. Platonov, S.I. Bogatyrenko, A.A. Minenkov
V.N. Karazin Kharkiv National University, Kharkiv, Ukraine
E-mail: lisovskiy@yahoo.com

In the present work, we measured breakdown and extinction curves of radio-frequency discharge in acetylene as well as dependences of active current, power and gas pressure on the discharge burning time, and also optical emission spectra. It was found that in the region of low acetylene pressures (to the left of the minimum of the breakdown curve), the discharge can cover only a part of the electrode surface. Immediately after the ignition of the discharge, due to the intense deposition of the polymer film and the formation of dust particles in the plasma volume, the gas pressure decreases sharply (by the factor of 2-5), while the active current and power increase and then reach saturation. In the discharge with intense polymerization, the lines of atomic and molecular hydrogen dominate in the emission spectrum of the discharge. The film deposited on the surface of the electrodes and the tube walls, as well as the dust particles formed, are amorphous, the maximum peak of XRD spectrum is observed at $2\theta = 18°$, and the light absorption by the deposited films is highest at 440 nm wavelength.

PACS: 52.80.Hc

INTRODUCTION

There is great scientific and industrial interest in the processes in gas-discharge plasma in hydrocarbons, particularly in acetylene, since it is widely used for deposition of polymer films [1, 2], diamond and diamond-like carbon (DLC) coatings [3 - 5], formation of carbon nanotubes, nanowalls, and other nanostructures [6 - 10]. For nanomaterials production the deposition in radio-frequency capacitive discharges (plasma-enhanced chemical vapor deposition) in carbon-containing gases (C_2H_2, CH_4, etc.) is one of the most promising technologies [6, 11]. This allows depositing nanomaterials on both substrates and electrodes, even if the deposited film is dielectric. However, in researches [6, 11] (and in the papers cited in them), attention is usually paid to characteristics of deposited coatings, as well as to the mass spectra of the resulting reaction products, but ignition, extinction and burning modes of the RF discharge are not studied. Therefore, the purpose of this work was an experimental study of ignition conditions, burning modes and properties of radio-frequency capacitive discharge in acetylene as an instrument for the synthesis of carbon nanomaterials.

1. EXPERIMENTAL

To study the RF capacitive discharge, a discharge chamber was used shown schematically in Fig. 1.

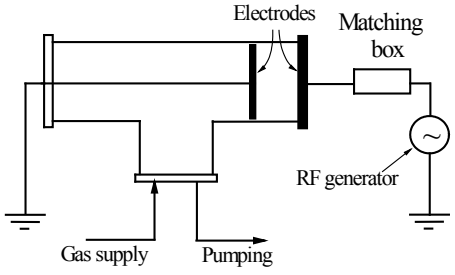

Fig. 1. Scheme of experimental setup

At the ends of the horizontal part of T-shaped glass discharge tube with internal diameter of 56 mm two flanges were placed, through which a voltage was applied to the electrodes. Grounded and potential electrodes with a diameter of 55 mm was located inside the discharge tube. The experiments were carried out at a distance between the electrodes of 20 mm in the range of applied RF voltages up to 2000 V. Through the flange located at the base of the vertical part the gas was injected and pumped out. A gas pressure gauge MKS Baratron of 10 Torr range was used to measure the gas pressure. The experiments were carried out in the range of acetylene pressure of 0.02…10 Torr.

An iHR-320 spectrometer (Horiba Scientific) with the wavelength range of 200…1000 nm was used to measure the emission spectra of the discharge plasma. This spectrometer includes a diffraction grating (1800 lines/mm) providing spectral resolution of 0.05 nm. The optical fiber of the spectrometer collected light emerging from the plasma discharge region immediately after the RF voltage was established between the electrodes. Due to the polymer film deposition on the tube walls, the intensity of all radiation lines passing through it decreases, therefore, we will not give spectral dependences for different moments of discharge operation. To analyze the spectra of molecular gases, we used the Pearse and Gaydon handbook [12].

During the RF discharge in acetylene operation a polymer film is deposited on the electrodes and the tube walls, and dust particles are formed in the plasma volume. For their analysis we used X-ray diffractometer XRD-6100 (Shimadzu), Scanning electron microscope (SEM) JEOL JSM-840, Transmission electron microscope (TEM) Selmi PEM-125K and LLG-uniSPEC2 Spectrophotometer (LLG Labware).

The electrodes in the discharge chamber were arranged vertically, that limited significantly the possibility of accumulation of the dust particles in the plasma volume.

2. EXPERIMENTAL RESULTS

First, let us consider the breakdown and extinction curves of RF capacitive discharge in acetylene shown in Fig. 2. The breakdown curve describes the conditions (gas pressure and applied RF voltage) under which gas breakdown occurs due to electron avalanches developing in an electric field, which ends with the creation of a stable burning discharge. Gas breakdown occurs when electrons in the applied electric field gain sufficiently

high energy and ionize the molecules with a frequency that is equal to the frequency of all electron losses due to diffusion and drift to the electrodes and the tube wall as well as electron attachment (in the case of electronegative gases) [13 - 18]. Breakdown curves measured in the studied gas at different distances between the electrodes make it possible to determine electron drift velocity [19 - 23], which is necessary for hydrodynamic modeling of processes in a gas-discharge plasma. From Fig. 2 it can be seen that the breakdown curve measured by us consists mainly of the diffusion-drift branch, which has the form of a parabola lying on its side (the names of different branches of the RF breakdown curves and processes that take part in the gas breakdown can be found in [24, 25]). And only at the lowest gas pressures and high RF voltages the transition to Paschen's branch is observed.

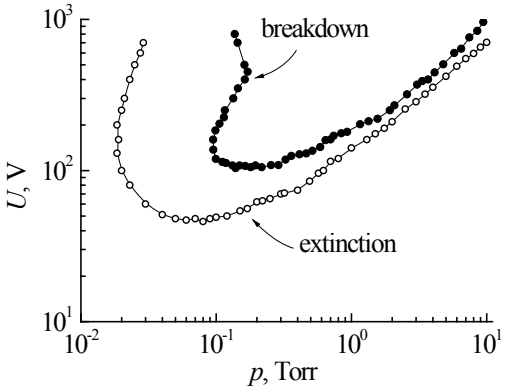

Fig. 2. Breakdown and extinction curves of RF discharge in acetylene

The extinction curve limits the area where infinite burning of the discharge previously created during gas breakdown is possible [26, 27]. On the extinction curve, there are branches similar to those of the breakdown curve. It is seen from Fig. 2 that both on the breakdown curve and on the extinction curve areas of ambiguous dependence of the breakdown RF voltage on the gas pressure are present. The presence of such a region of ambiguity in the breakdown curve allows, under certain conditions, to ignite the discharge, lowering the RF voltage across the electrodes. At the same time, at low gas pressures it is possible to quench the discharge by increasing the RF voltage. Note that in the area of gas pressure to the left of the turning point (the point where the derivative of the RF breakdown voltage of the gas reaches infinity), the RF discharge may not cover the entire surface of the electrodes, it glows in the form of a plasma cord. This situation is also observed in acetylene, when at low pressures the discharge glow appears only in the lower part of the tube, and the rest of the chamber is occupied by the afterglow. Apparently, such a downward shift of the plasma region is due to the fact that the dust particles formed in the discharge volume drop under the action of gravity and are concentrated in the lower part of the discharge chamber. In this part of the discharge, only a small ambipolar electric field holds them [28], preventing them from falling onto the tube wall (unlike the horizontal arrangement of electrodes, when dust particles are held in the plasma volume by a strong electric field near the electrode sheaths [29 - 32]). Thus, only small dust particles can be held in the plasma volume of our discharge chamber, and large dust clusters and parts of the film detached from the electrodes falls on the surface of the tube. The conditions when the discharge can occupy only a part of the chamber are not suitable for its effective use, for example, during the deposition of a polymer film, since the properties of the film deposited in the plasma region and in the afterglow will differ. Therefore, the RF capacitive discharge application in plasma technologies requires measuring the breakdown and, especially, extinction curves in the discharge chamber used.

Next, consider the emission spectra of the plasma region of the RF discharge. Fig. 3 shows the emission spectra at acetylene pressure of 0.05 Torr for various RF voltages. This figure shows that with increasing RF voltage, the intensities of all emission lines increase. The Balmer line of atomic hydrogen H_α and the H_2 molecule lines dominate; however, the lines of C_2, C_3, and CH molecules are also intense. Using the reference book [12], one can find lines of more complex molecules (for example, benzene), but their intensity is low. At higher acetylene pressures (Fig. 4 shows the case for 1 Torr), the intensity of the molecular lines of C_2, C_3, and CH decreases, and the emission spectrum of the discharge plasma is almost completely determined by the lines of atomic and molecular hydrogen.

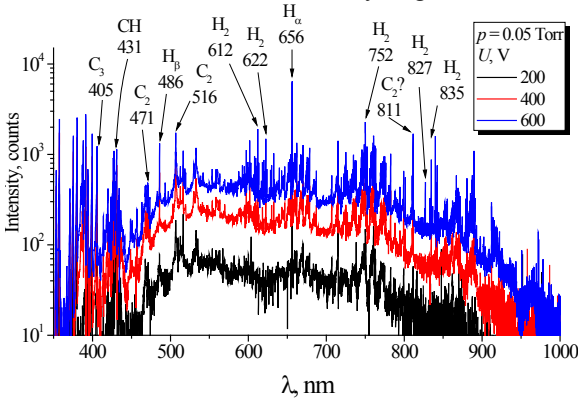

Fig. 3. Optical emission spectrum from the discharge center at acetylene pressure of 0.05 Torr and various values of RF voltage

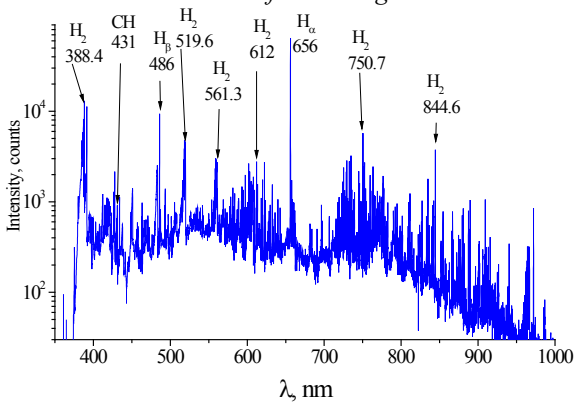

Fig. 4. Optical emission spectrum from the discharge center at acetylene pressure of 1 Torr and RF voltage of 1800 V

We observed that immediately after the breakdown the gas pressure in RF capacitive discharge in acetylene rapidly decreases by a factor of 2-5 (depending on the magnitude of the initial pressure and the gas flow rate

into the chamber) and is stabilized within 0.5…1 min (Fig. 5). It should be mentioned that before filling with acetylene the discharge chamber was pumped out by a turbomolecular pump to the base pressure of about 10^{-5} Torr, then acetylene was fed up to the pressure of 0.015…0.1 Torr, and then the pressure in the chamber was set adjusting the pumping speed using a vacuum valve. Apparently, the rate of acetylene consumption by the polymerization process may be higher than the rate of gas flow into the chamber. This explains the fact that in the optical emission spectrum of acetylene plasma, the lines of the molecules C_2, C_3, and CH are significantly weakened. A sharp decrease in pressure was usually observed in closed chambers, without gas feeding and pumping [33]. In flow chambers, the pressure may remain unchanged. In fact, the discharge plasma, in which an intensive polymerization takes place (both with the film deposition on the walls and with the dust particles growth in the plasma volume), can play the role of a pump that actively removes the gas molecules from the chamber.

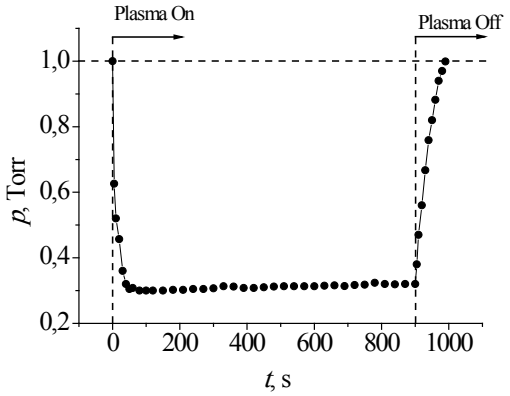

Fig. 5. The dependence of the gas pressure on the time after the ignition. The initial acetylene pressure is 1 Torr, the RF voltage is 900 V

Immediately after the discharge ignition, if the RF power is kept fixed, the value of the RF voltage varies slightly, but on average remains approximately equal to 900 V (Fig. 6). The phase angle between voltage and current is first 84°, then decreases to 75°, that is, the RF discharge becomes more resistive with time. This occurs apparently due to the formation of the dust particles in the plasma volume absorbing free electrons. To compensate for these electron losses, the RF voltage across the plasma volume rises, the electron temperature increases, causing rise of ionization rate.

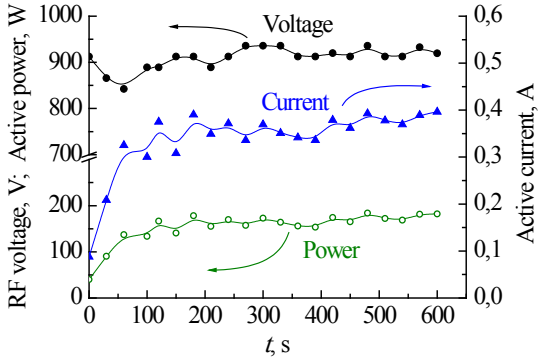

Fig. 6. Dependencies of RF voltage on the electrodes, active current and active power on the discharge burning time. The initial acetylene pressure is 1 Torr

The polymer films deposited on the electrodes, and the dust particles deposited to the tube walls were analyzed. Fig. 7 shows TEM pictures of the dust particles collected from the tube wall. Their shape is close to spherical, and the diameter reaches several hundred nanometers. These dust particles can be clustered. But, as mentioned above, in our discharge chamber with vertically arranged electrodes, large particles or clusters cannot be kept in the plasma volume due to the small amount of voltage drop across the wall layer. Therefore, in TEM images (presented in the figure, as well as in a number of others obtained by us) there are no dust particles with a diameter greater than 1 μm. From the bottom picture in Fig. 7, it can be seen that the polymer film deposited on the electrodes is not homogeneous, but includes many polymer clusters whose diameter is close to 10 nm.

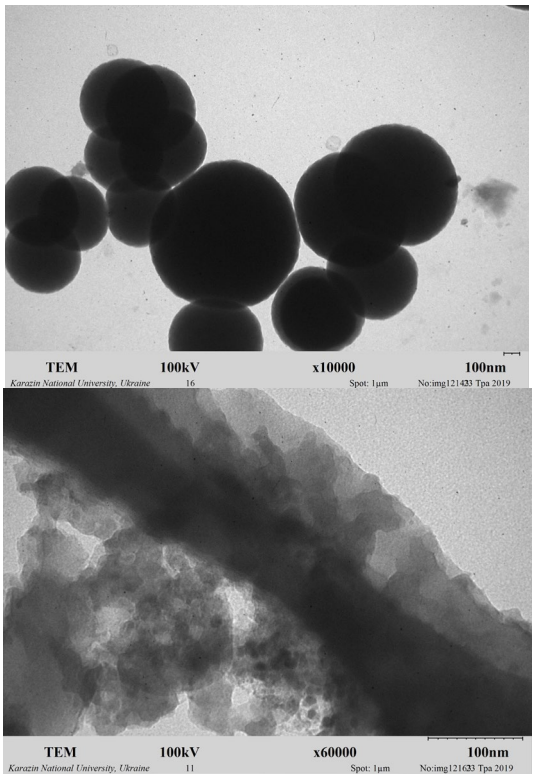

Fig. 7. TEM images of dust particles and polymer film formed with acetylene pressure of 1 Torr and RF voltage of 1800 V

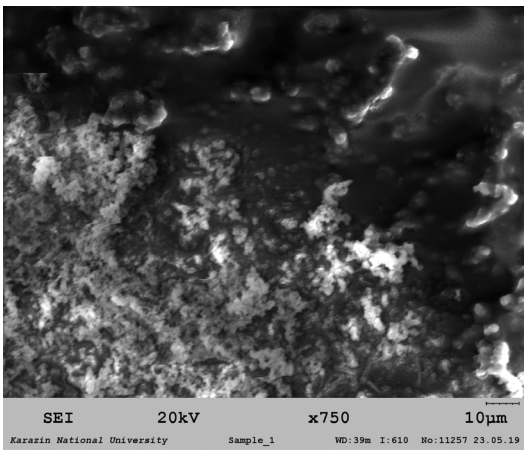

Fig. 8. SEM image of clusters of dust particles deposited on the tube wall at acetylene pressure of 1 Torr and an RF voltage of 1800 V

Fig. 8 shows SEM image of clusters of dust particles that were formed in the plasma volume and then deposited on the tube wall. Lack of resolution in the SEM images is caused by dielectric nature of the studied deposits that leads to eclectic charging of their surface disturbing the SEM image.

It is interesting that the dust particles and the clusters cover not only the lower and side surfaces of the discharge tube (where the dust particles can drop due to gravity), but also the upper part of the tube. Apparently, the only force that can lift a dust particle up, against gravity, is the ion drag force [34 - 36]. The flows of positive ions move from the plasma not only to the electrodes through the electrode layers. Fast electrons go to the dielectric walls of the tube, charge them to a negative potential of about 10…20 V, which leads to the flow of positive ions to the walls of the tube through the wall layer. Dust particles formed in the plasma volume are pushed by positive ions to the surface layer. In this layer, the electron concentration is low (there are few fast electrons capable of overcoming the ambipolar potential difference in the layer, and cold electrons are reflected from the layer back to the plasma). Dust particles trapped in the plasma volume are usually negatively charged. But, being pushed by ions into the wall layer, dust particles can acquire a positive charge and will continue to be attracted to the negatively charged wall of the tube, even against gravity.

The films deposited on the electrodes, as well as on the tube walls, were investigated using the LLG – uniSPEC2 spectrophotometer and the iHR – 320 spectrometer. UV, visible and near-IR light was transmitted through both films deposited on glass substrates and through suspension of the film in toluene. Both methods (films and solutions) gave similar results (for example, Fig. 9). The lowest light transmission (respectively, the highest absorption) is observed at about 440 nm for the films deposited on both the electrode and the tube wall in contact with the near-electrode layers. In the plasma region, as mentioned above, clusters of dust particles, which create an almost opaque layer, drop onto the tube wall. However, even for this case, Fig. 9 shows the presence of a small minimum of transmission, which indicates the similarity of the composition of both dust particles and the polymer film.

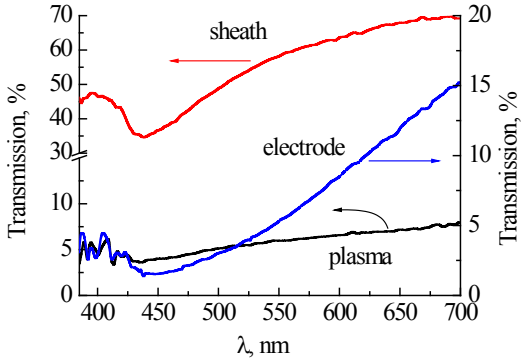

Fig. 9. The dependence of visible light transmission on wavelength for the films deposited on the electrodes, as well as on the tube walls in the plasma region and in the near-electrode sheaths. The films were deposited at initial acetylene pressure of 0.5 Torr and RF voltage of 1500 V

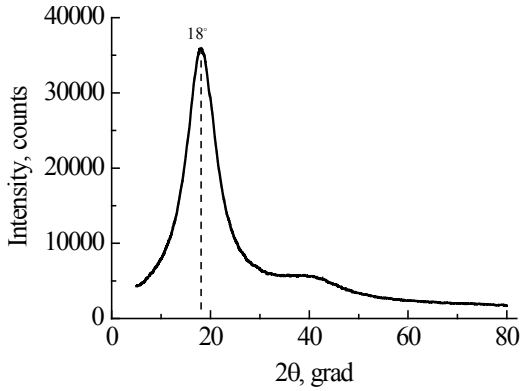

Fig. 10. XRD pattern of polymer film and dust particles formed in an RF discharge in acetylene

Additional information about the material of deposited polymer films was obtained using X-ray diffraction (XRD, Fig. 10). It was found that the XRD pattern of the polymer film and the dust particles formed in the acetylene RF discharge has a broad peak at $2\theta = 18°$. The high peak width indicates that the deposited film is amorphous. It can be assumed that the polymer film produced in the acetylene plasma is polyacetylene. However, for polyacetylene, light absorption has a maximum at about 700 nm [37], while for our film in this part of the spectrum absorption is minimal. And the pure polyacetylene XRD pattern has a maximum at $2\theta = 25°$ [38]. In addition, a lot of polymers has a maximum light absorption at 400…450 nm (see, for example, [39 - 41]). Therefore, additional studies are needed to clarify the composition of the polymer film obtained by us in the RF capacitive discharge in acetylene.

CONCLUSIONS

In this work, we investigated the ignition and extinction of radio-frequency discharge in acetylene, the time dependences of gas pressure, active current and power, as well as optical emission spectra of the plasma. It is shown that, in the region of acetylene pressures to the left of the minimum of the breakdown curve, the discharge may not fill the entire chamber that can make problems for polymer film deposition. It was observed that the discharge with intense polymerization can play the role of a plasma pump, leading to a significant (2-5 fold) decrease in the gas pressure. Using X-ray diffraction, it was obtained that the polymer film is amorphous with a broad peak at $2\theta = 18°$.

ACKNOWLEDGMENT

We are grateful to our colleagues O. Zhytniakivska, U. Tarabara, K. Vus, and G.P. Gorbenko for their help in measuring with a spectrophotometer.

REFERENCES

1. Eds. P.J. Stang and F. Diederich. *Modern Acetylene Chemistry* // Wiley, Weinheim, 2008, 531 p.
2. S.C. Rasmussen. *Acetylene and Its Polymers. Springer*. Cham, Switzerland, 2018, 136 p.
3. J.W. Zou, K. Schmidt, K. Reichelt, and B. Dischler. The properties of a-C:H films deposited by plasma decomposition of C_2H_2 // *J. Appl. Phys*. 1990, v. 67, № 1, p. 487-494.

4. J. Robertson. Diamond-like amorphous carbon // *Materials Science and Engineering*. 2002, v. 37, № 4-6, p. 129-281.
5. M. Frenklach, H. Wang. Detailed surface and gas-phase chemical kinetics of diamond deposition // *Phys. Rev. B*. 1991, v. 43, № 2, p. 1520-1545.
6. A. Thapa, S. Neupane, R. Guo, K.L. Jungjohann, D. Pete, W. Li. Direct growth of vertically aligned carbon nanotubes on stainless steel by plasma enhanced chemical vapor deposition // *Diamond & Related Materials*. 2018, v. 90, p. 144-153.
7. A.T. Yousefi. Nanocomposite-Based *Electronic Tongue: Carbon Nanotube Growth by Chemical Vapor Deposition and Its Application.* Springer International Publishing, Cham, Switzerland. 2018, 101 p.
8. S. Suzuki (Ed.). *Syntheses and Applications of Carbon Nanotubes and Their Composites.* In Tech, Rijeka, Croatia. 2013, 537 p.
9. W. Fan, L. Zhang, T. Liu. *Graphene-Carbon Nanotube Hybrids for Energy and Environmental Applications.* Springer, Singapore. 2017, 104 p.
10. S. Ghafouri, S. Abdijahed, Sh. Farivar, et al. Study on Physio-chemical Properties of Plasma Polymerization in C2H2/N2 Plasma // *Scientific Reports*. 2017, v. 7, № 1, p. 1-16.
11. J. Benedikt. Plasma-chemical reactions: low pressure acetylene plasmas // *J. Phys. D: Appl. Phys*. 2010, v. 43, № 4, p. 043001.
12. R.W.B. Pearse, A.G. Gaydon. *The identification of molecular spectra.* Chapman & Hall, London, 1950.
13. I. Korolov and Z. Donko. Breakdown in hydrogen and deuterium gases in static and radio-frequency fields // *Phys. Plasmas*. 2015, v. 22, p. 093501.
14. V.A. Lisovskiy. Criterion for microwave breakdown of gases // *Technical Physics*. 1999, v. 44, № 11, p. 1282-1285.
15. V. Lisovskiy, S. Martins, K. Landry, D. Douai, J.-P. Booth, V. Cassagne, V. Yegorenkov. The effect of discharge chamber geometry on the ignition of low-pressure rf capacitive discharges // *Physics of Plasmas*. 2005, v. 12, № 9, p. 093505.
16. V. Lisovskiy, J.-P. Booth, K. Landry, D. Douai, V. Cassagne, V. Yegorenkov. Similarity Law for RF breakdown // *Europhysics Letters*. 2008, v. 81, № 1, p. 15001.
17. V.A. Lisovskiy, N.D. Kharchenko, V.D. Yegorenkov. Modes of longitudinal combined discharge in low pressure nitrogen // *J. Phys. D: Appl. Phys*. 2008, v. 41, № 12, p. 125207.
18. V.A. Lisovskiy, N.D. Kharchenko, V.D. Yegorenkov. Low-pressure gas breakdown in longitudinal combined electric fields // *J. Phys. D: Appl. Phys*. 2010, v. 43, № 42, p. 425202.
19. V.A. Lisovskiy. Determination of electron transport coefficients in argon from ignition curves of rf and combined low-pressure discharges // *Technical Physics Letters*. 1998, v. 24, № 4, p. 308-310.
20. V.A. Lisovskiy, V.D. Yegorenkov. Electron-drift velocity determination in CF_4 and SF_6 in a strong electric field from breakdown curves of low-pressure RF discharge // *J. Phys. D*: *Appl. Phys*. 1999, v. 32, № 20, p. 2645-2648.
21. V. Lisovskiy, J.-P. Booth, K. Landry, D. Douai, V. Cassagne, V. Yegorenkov. Electron drift velocity in N_2O in strong electric fields determined from rf breakdown curves // *J. Phys. D: Appl. Phys*. 2006, v. 39, № 9, p. 1866-1871.
22. V. Lisovskiy, J.-P. Booth, K. Landry, D. Douai, V. Cassagne, V. Yegorenkov. Electron drift velocity in argon, nitrogen, hydrogen, oxygen and ammonia in strong electric fields determined from rf breakdown curves // *J. Phys. D: Appl. Phys*. 2006, v. 39, № 4, p. 660-665.
23. V. Lisovskiy, S. Martins, K. Landry, D. Douai, J.-P. Booth, V. Cassagne. Electron drift velocity in NH_3 in strong electric fields determined from rf breakdown curves // *J. Phys. D: Appl. Phys*. 2005, v. 38, № 6, p. 872-876.
24. V.A. Lisovskiy, V.D. Yegorenkov. RF breakdown of low-pressure gas and a novel method for electron drift velocity determination in gases // *J. Phys. D: Appl. Phys*. 1998, v. 31, № 23, p. 3349-3357.
25. V. Lisovskiy, V. Yegorenkov, J.-P. Booth, K. Landry, D. Douai, V. Cassagne. Electron drift velocity in SF6 in strong electric fields determined from rf breakdown curves // *J. Phys. D: Appl. Phys*. 2010, v. 43, № 38, p. 385203.
26. V. Lisovskiy, J.-P. Booth, S. Martins, K. Landry, D. Douai, V. Cassagne. Extinction of RF capacitive low-pressure discharges // *Europhysics Letters*. 2005, v. 71, № 3, p. 407-411.
27. V. Lisovskiy, N. Kharchenko, V. Yegorenkov. Longitudinal combined discharge extinction in low pressure nitrogen // *Vacuum*. 2008, v. 83, № 4, p. 724-726.
28. V.A. Lisovskiy, N.D. Kharchenko, V.D. Yegorenkov. Radial structure of low pressure rf capacitive discharges // *Vacuum*, 2010, v. 84, № 1, p. 782-791.
29. P. Chabert, N. Braithwaite. *Physics of Radio-Frequency Plasmas.* Cambridge University Press, Cambridge, 2011.
30. V. Lisovskiy, V. Yegorenkov. Double layer onset inside the near-electrode sheath of a RF capacitive discharge in oxygen // *Vacuum*. 2006, v.80, p. 458-467.
31. V.A. Lisovskiy. Features of the alpha - gamma transition in a low-pressure rf argon discharge // *Technical Physics*. 1998, v. 43, № 5, p. 526-534.
32. V.A. Lisovskiy, V.D. Yegorenkov. Alpha–gamma transition in RF capacitive discharge in low-pressure oxygen // *Vacuum*. 2004, v. 74, p. 19-28.
33. H. Yasuda. *Plasma Polymerization.* New York: Academic Press, 1985, 376 p.
34. S. Khrapak, G. Morfill. Basic Processes in Complex (Dusty) Plasmas: Charging, Interactions, and Ion Drag Force // *Contrib. Plasma Phys*. 2009, v. 49, № 3, p. 148-168.
35. A.V. Ivlev, S.K. Zhdanov, S.A. Khrapak, G.E. Morfill. Ion drag force in dusty plasmas // *Plasma Phys. Control. Fusion*, 2004, v. 46, p. B267-B279.
36. I. Denysenko, M.Y. Yu, L. Stenflo, S. Xu. Ion drag force in plasmas at high electronegativity // *Phys. Rev. E*. 2005, v. 72, № 1, p. 016405.

37. H. Shirakawa, T. Ito, S. Ikeda. Raman scattering and electronic spectra of poly (acetylene) // *Polymer J.* 1973, v. 4, № 4, p. 460-462.
38. J.C.W. Chien. *Polyacetylene: Chemistry, Physics, and Material.* New York: Academic Press, 1984, 634 p.
39. B.W. Chieng, N.A. Ibrahim, W.M.Z.W. Yunus, M.Z. Hussein. Poly (lactic acid) / Poly (ethylene glycol) Polymer Nanocomposites: Effects of Graphene Nanoplatelets // *Polymers*. 2014, v.6, p. 93-104.
40. M.G. Manjunatha, A.V. Adhikari, P.K. Hegde, C.S.S. Sandeep, R. Philip. Optical characterization of a new donor–acceptor type conjugated polymer derived from 3,4-diphenylthiophene // *J. Mater. Sci*. 2009, v. 44, p. 6069-6077.
41. N. Jaballah, K. Hriz, M. Chemli, J.-L. Fave, and M. Majdoub. New Semiconducting Poly(arylene sulfide)s: Synthesis, Characterization, and Optical Properties // *International Journal of Polymer Anal. Charact*. 2014, v. 19, p. 594-610.

Article received 03.06.2019

ЗАЖИГАНИЕ И СВОЙСТВА ВЧ-ЕМКОСТНОГО РАЗРЯДА В АЦЕТИЛЕНЕ

В.А. Лисовский, С.В. Дудин, П.П. Платонов, С.И. Богатыренко, А.А. Миненков

Измерены кривые зажигания и погасания, зависимости активных тока, мощности и давления газа от времени горения разряда, а также спектры излучения высокочастотного разряда в ацетилене. Получено, что в области низких давлений ацетилена (слева от минимума кривой зажигания) разряд может покрывать только часть поверхности электродов. Сразу после зажигания разряда из-за интенсивного осаждения полимерной пленки и образования пылевых частиц в плазменном объеме резко (в 2-5 раз) уменьшается давление газа, а активные ток и мощность возрастают и затем выходят на насыщение. В процессе интенсивной полимеризации в спектре излучения разряда доминируют линии атомарного и молекулярного водорода. Осаждаемая на поверхность электродов и стенок трубки пленка, а также формирующиеся пылевые частицы являются аморфными, для них максимальное дифракционное рассеяние рентгеновских лучей наблюдается при $2\theta = 18°$, а поглощение видимого света является наибольшим при 440 нм.

ЗАПАЛЮВАННЯ ТА ВЛАСТИВОСТІ ВЧ-ЄМНІСНОГО РОЗРЯДУ В АЦЕТИЛЕНІ

В.О. Лісовський, С.В. Дудін, П.П. Платонов, С.І. Богатиренко, О.О. Мінєнков

Виміряні криві запалювання та згасання, залежності активних струму, потужності та тиску газу від часу горіння розряду, а також спектри випромінювання високочастотного розряду в ацетилені. Отримано, що в області низьких значень тиску ацетилену (зліва від мінімуму кривої запалювання) розряд може покривати тільки частину поверхні електродів. Відразу після запалювання розряду через інтенсивне осадження полімерної плівки і утворення пилових частинок у плазмовому об'ємі різко (в 2-5 разів) зменшується тиск газу, а активні струм і потужність зростають і потім виходять на насичення. У процесі інтенсивної полімеризації в спектрі випромінювання розряду домінують лінії атомарного і молекулярного водню. Плівка, що осаджується на поверхню електродів і стінок трубки, а також пилові частинки, що формуються, є аморфними, для них максимальне дифракційне розсіювання рентгенівських променів спостерігається при $2\theta = 18°$, а поглинання видимого світла є найбільшим при 440 нм.